JCTC Journal of Chemical Theory and Computation

Molecular Dynamics Simulations of HIV-1 Protease Suggest Different Mechanisms Contributing to Drug Resistance

Florian Wartha, Anselm H. C. Horn, Heike Meiselbach, and Heinrich Sticht*

Abteilung Bioinformatik, Institut für Biochemie, Emil-Fischer-Zentrum, Friedrich-Alexander-Universität Erlangen-Nürnberg, Fahrstrasse 17, D-91054 Erlangen, Germany

Received November 26, 2004

Abstract: A major problem in the antiretroviral treatment of HIV-infections with protease-inhibitors is the emergence of resistance, resulting from the occurrence of distinct mutations within the protease molecule. In the present work molecular dynamics simulations of an active-site mutation (D30N) and a nonactive-site mutation (N88S) of HIV-1 protease that both directly confer resistance to the protease inhibitor Nelfinavir but not to Amprenavir were performed and compared to wild-type HIV-protease. A decreased interaction energy between protease and Nelfinavir was observed for the D30N mutant giving a plausible explanation for resistance, while the N88S mutation did not significantly affect the interaction energies in the bound form. Structural analysis including both ligand-bound and unliganded HIV-1 proteases revealed that the free N88S mutant protease shows significant differences in its hydrogen bonding pattern compared to free or Nelfinavir-bound wild-type protease. In particular, Asp30 forms more frequently a hydrogen bond with Ser88 in the unbound N88S mutant thus interfering with the Asp30-Nelfinavir interaction. These findings suggest that different molecular mechanisms contribute to resistance in active-site and nonactive-site mutants and propose a mechanism for the N88S mutant that is based on a shift of the conformational equilibrium of the unbound protease.

Introduction

The global spread of the human immunodeficiency virus (HIV) causing the acquired immune deficiency syndrome (AIDS) has evolved into an immense health problem with total estimated infection numbers ranging from 34 to 46 million people.[1] The HIV-1 protease is essential for replication and assembly of the virus, and the inactivation of the HIV-1 protease leads to the production of noninfectious viral particles.[2] The idea of inhibiting viral replication by disturbing the protease function has led to the development of a class of drugs known as protease inhibitors (PI).[3] Modern HIV combination therapies, referred to as "Highly Active Anti-Retroviral Therapy" (HAART), attack the virus with a combination of one protease inhibitor and two reverse transcriptase (RT) inhibitors.[4] The extensive use of antiretrovirals, however, has led to the emergence of resistant virus variants that possess various degrees of cross-resistance due to mutations.[5]

Mutations can either occur at active-site or nonactive-site locations in HIV-1 protease (Figure 1A) and can also confer different levels of resistance. Primary mutations directly confer resistance to one or more protease inhibitors, whereas secondary mutations only contribute to resistance and often occur together with primary ones or in synergistic form with other secondary mutations. Active-site mutations are exclusively primary ones, but not all primary mutations are necessarily limited to the active-site (e.g. the nonactive site mutations at sequence positions 46, 88 and 90 can also directly confer resistance[6]).

The mechanism of active-site mutations can frequently be rationalized in structural terms in which resistance is directly

* Corresponding author phone: +49−9131−8524614; fax: +49−9131−8522485; e-mail: h.sticht@biochem.uni-erlangen.de.

10.1021/ct049869o CCC: $30.25
Published on Web 02/04/2005

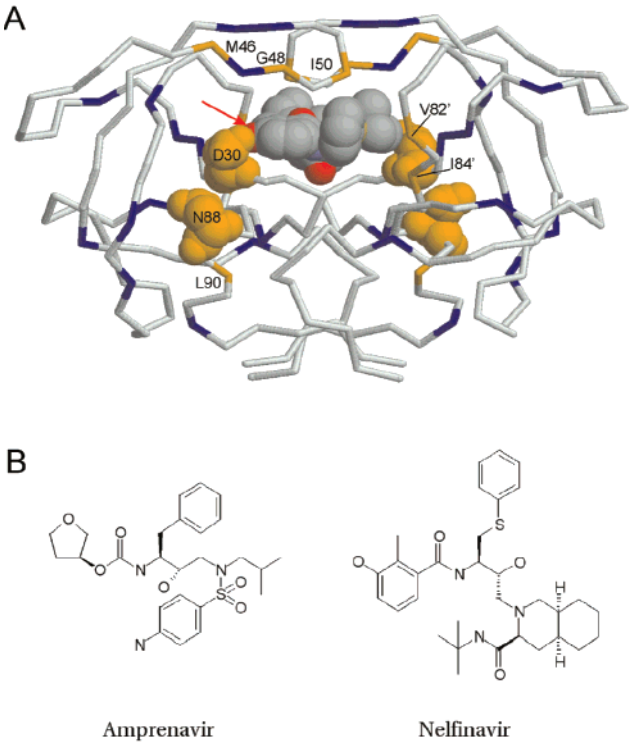

Figure 1. A) Structure of the dimeric HIV-1 protease with bound Nelfinavir showing the most common primary and secondary HIV-1 protease drug-resistance causing mutations. Only the backbone-atoms of a wild-type HIV protease are depicted, whereas the protease inhibitor Nelfinavir is represented in space-filled representation with standard cpk coloring. Primary mutations (30, 46, 48, 50, 82, 84, 88 and 90) are drawn in orange, secondary mutations (10, 20, 24, 32, 33, 36, 47, 53, 54, 63, 71, 73, 77 and 93) in blue. Primary mutations are labeled in one of the subunits, and the two mutations studied here (D30 and N88) are shown in a space-filled representation. A red arrow indicates the hydrogen bond between the Asp30 side chain of one subunit and the phenyl oxygen of Nelfinavir which is discussed in the text. B) HIV-1 protease inhibitors used in this study. The chemical formulas are depicted in Lewis representation. Amprenavir susceptibility is maintained after D30N and N88S mutation, whereas both mutations confer resistance to Nelfinavir.

associated with a change of the contacts and thus the interaction energy between drug and target.[7] In contrast, the mechanism of nonactive-site mutations, influencing binding from distal locations, is not satisfyingly understood. These mutations are able to affect the enzymatic activity via mechanisms that have for example been related to differences in the conformational flexibility[8] or to the alteration of the binding site geometry through the accumulation of mutations within the core of the protease, suggesting that nonactive-site mutations can even represent the primary source of resistance.[9]

Resistance can either be assessed from genotypic assays based on the detection of mutations associated with the resistance or from phenotypic assays by measurement of the virus sensibility to increasing concentration of antiretroviral substances.[10] The correlation between genotypic mutations and phenotypic resistance, however, is not fully understood,[11,12] and therefore genotypic testing needs to rely on comprehensive statistical data of known drug-resistance mutations.[13] In contrast, phenotypic assays directly give information about resistance, but they are experimentally demanding and difficult to standardize.[14] One disadvantage of both genotypic and phenotypic assays is that they do not provide a molecular mechanistical explanation for the emergence of resistance which would be extremely useful for developing more effective and longer lasting treatment strategies. In this context, computational studies of the dynamics and energetics of HIV-1 protease and protease-inhibitor complexes can give valuable insight into the molecular mechanism of mutations in conferring drug resistance.[8,15,16]

In the present study, two primary mutations (D30N, N88S) which often occur during treatment of HIV-infected patients[17−19] were analyzed using molecular dynamics simulations and subsequent structural and energetic analysis. D30N constitutes an active-site mutation, that reduces Nelfinavir (NLF) susceptibility by 5−20-fold[6] and is able to do so without any further major mutations.[20] Although N88S is a nonactive-site mutation, it has the remarkable ability to cause NLF-resistance even in the absence of active-site mutations.[6] Similar to D30N, the N88S mutation also causes resistance selectively for NLF (Figure 1B). Therefore studies of wild-type (WT) and mutant proteases in complex with other inhibitors (e.g. Amprenavir, APV) can serve as a control in both cases. To take into account that the mechanisms underlying resistance caused by the D30N and N88S mutation might differ substantially, the dynamics of the unliganded wild-type and mutant proteases were characterized here as well.

Methods

Preparation of Starting Structures. The starting structures of the protease-drug and protease-substrate complexes were taken from following entries available in the Protein Data Bank (PDB[21]): 1HPV for protease complexed with APV,[22] 1OHR for protease + NLF[23], and 4HVP for the protease + substrate-analogue.[24] Since no high-resolution crystal structure of an unliganded HIV-1 protease is available, the starting structures of the unbound forms were generated by removing an inhibitor from the APV-bound form, thus following the common strategy applied in previous studies.[15,25]

The protease sequence of the 1HPV and 1OHR-entries was taken as a wild-type sequence. The protease of the 4HVP file, containing one secondary mutation (L63P) and four polymorphisms (K14R, S37N, R41K, I64V), was modified by mutating the affected residues to the WT-sequence as described previously[26,27] using Sybyl 6.9.[28] N88S and D30N mutant structures were also generated using Sybyl. According to the strategy outlined by Piana et al.,[8] the structure of the substrate was generated from a crystal structure (4HVP) containing a substrate analogue (MVT-101) by replacing the uncleavable CH_2NH linkage between Nle-Nle by a Met-Met peptide bond, leading to a substrate (Thr-Ile-Met-Met-Gln-Arg) that contains a natural cleavage site for the HIV-1 protease, the so-called p2/NC site.[29]

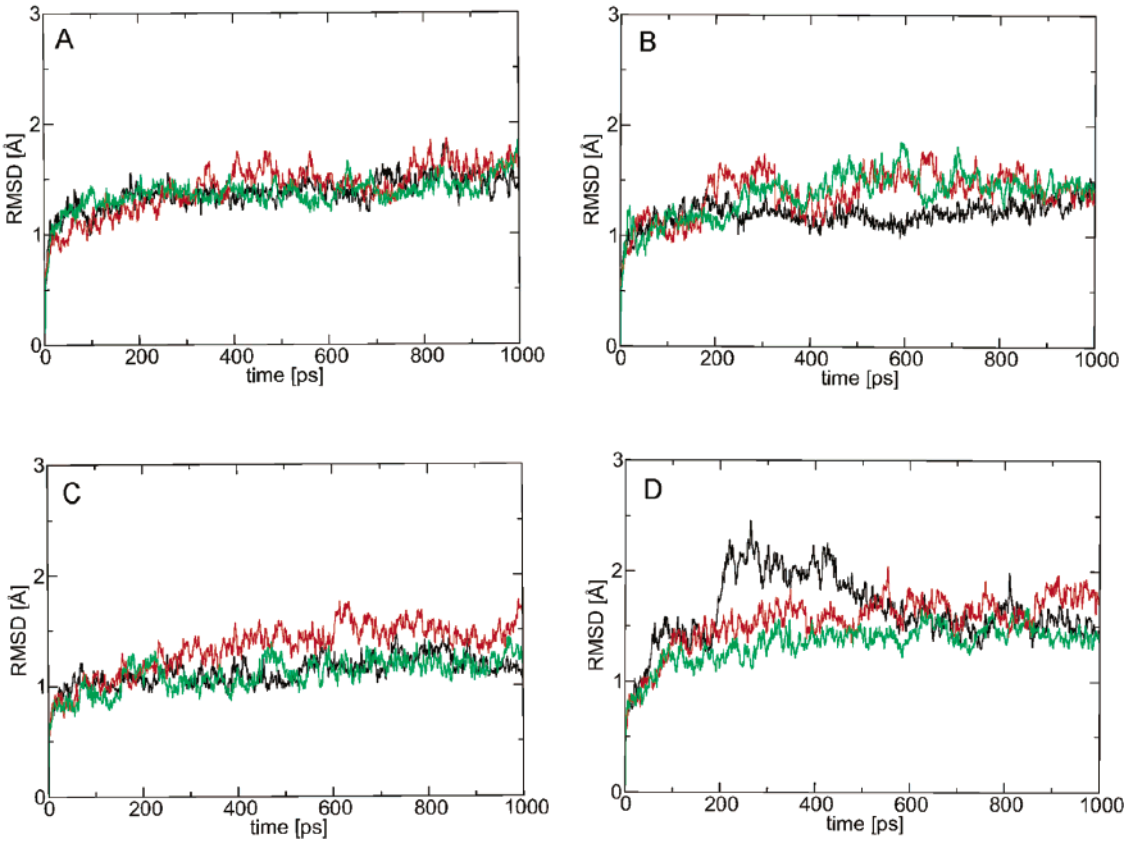

Figure 2. Root-mean-square deviation (RMSD) to the starting structure as a function of simulation time. Proteases liganded with A) substrate, B) APV, C) NLF, D) unliganded. Black: WT-protease; red: D30N; green: N88S. Calculations were performed for the backbone atoms of the respective structure versus the backbone atoms of the respective simulation's starting structure (excluding drug/substrate).

The simulations were performed under physiological pH conditions which required ensuring the correct protonation state of ionizable groups. In particular, one of the aspartates (D25) of the catalytic site exhibits an increased pK_a value of 5.2 in the inhibitor-bound protease,[30] while no increased pK_a was reported for the free form of the protease (pK_a = 4.5[31]). Therefore, a fully deprotonated active site should be prevalent at a physiological pH, and thus this protonation state was used throughout the simulations. However, to ensure that the results of the simulations do not critically depend on the protonation state, a 1 ns control simulation of a NLF-bound HIV-1 protease with a protonated carboxylate oxygen of Asp25 was also performed.

Parameter Generation for Inhibitors. The initial coordinates of APV and NLF were extracted from the 1OHR and 1HPV pdb files. ArgusLab[32] was utilized to add missing hydrogens, ensure correct protonation states and perform an initial geometry optimization using the Universal Force Field method.[33] The resulting structures were then further geometry optimized using the semiempirical molecular orbital Hamiltonian AM1[34] as implemented in Vamp.[35] The structures thus obtained were subjected to three consecutive geometry optimizations with Gaussian98[36] using the ab initio methods HF/MIDI!, B3LYP/6-31G(d) and HF/6-31G(d). For all four quantum mechanical geometry optimizations the stationary points found were ensured to be true minima by the calculation of the vibrational frequencies. For the two final structures of APV and NLF the atomic charges were then obtained following the established procedure[37,38] by fitting the charges to the HF/6-31G(d) computed electrostatic potential using the "antechamber" tool from the AMBER program suite.

Molecular Dynamics Simulations and Analysis. All MD simulations presented in this work were performed by using the AMBER 7.0 suite of programs[39] with the Cornell et al. force field (ff99).[40,41] For the organic compounds APV and NLF the general AMBER force field (gaff)[42] was used. An appropriate number of Cl^- counterions was added to neutralize the system, and afterward the molecules were solvated in a box of water, using the TIP3P water model[43] with at least 10.0 Å of water around every atom of the solute.

All structures were minimized first by using the sander module in AMBER with an atom-based 10 Å cutoff on electrostatic interactions, using a constant dielectric for the electrostatic interactions, $\epsilon = 1$. Particle Mesh Ewald summation[44] was used to calculate the long-range electrostatic interactions during minimization and during molecular dynamics.

The minimization procedure was split into three different parts. First the solvent was allowed to relax while restraining the protein atoms to their original position with a force constant of 500 kcal mol^{-1} $Å^{-2}$. Afterward additional relaxation of the protein side chains was allowed by restraining only the backbone atoms before in a final minimization all restraints were removed. The minimizations

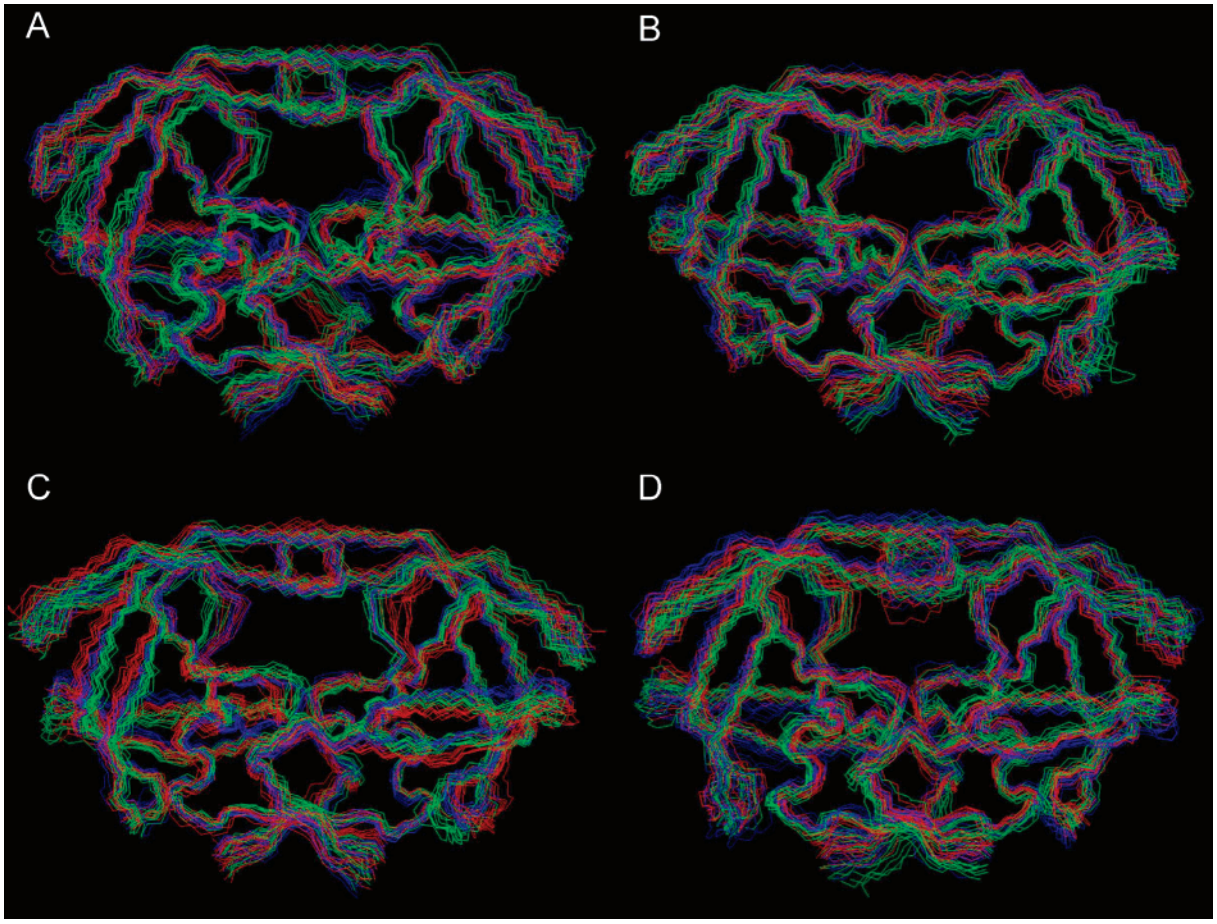

Figure 3. Fitted backbone overlay of proteases. Eleven structures of WT and both mutant proteases were taken in 100 ps intervals from the trajectory of the proteases liganded with A) substrate, B) APV, C) NLF, D) unliganded. WT: blue; D30N: red and N88S: green. All structures are backbone-fitted on the first structure of the wild-type simulations. The ligands are not shown for clarity.

consisted of 250 steps of steepest descent followed by 250 or 7250 steps of conjugate gradient minimization, respectively.

MD simulations were carried out thereafter, using a dielectric constant for the electrostatic interactions of $\epsilon = 1$ and a time-step of 1 fs. The temperature of the system was raised gradually from 50 to 298 K in 10 ps. Subsequently, 1 ns MD simulations with standard NPT conditions were performed for data collection, resulting in a total of 1000 snapshots. The SHAKE procedure[45] was used to constrain all bonds involving hydrogens. An 8.5 Å cutoff was used for the nonbonded interactions which were updated every 15 steps. For the visualization and structural analysis of the programs RasMol,[46] Sybyl 6.9,[28] IsisDraw,[47] AMBER,[39] and X-PLOR[48] were used.

Results and Discussion

Stability of the Trajectories and Properties of the Global Structure. A qualitative examination of the trajectories obtained from 12 MD simulations performed in the presence of different mutants and inhibitors (Figure 2) shows that all systems deviated to a quite similar extent from their starting structures resulting in a backbone RMSD of approximately 1.2−1.8 Å after 1 ns. The magnitude of the fluctuations is in the same range as those observed for the same time scale in recent simulations of HIV-1 protease.[15,16,49] Thus, one can conclude that the simulation runs produced stable trajectories which should provide a suitable basis for the subsequent analyses.

The structure and conformational variability of the ensembles obtained over the simulation time (Figure 3) reveals that both the structures and the magnitude of the fluctuations are quite similar for all 12 systems studied. The observation that neither mutations nor different ligands lead to larger structural changes is consistent with the findings of Zoete et al.[50] who showed that 73 crystal structures of HIV-1 protease do not differ significantly in their geometry, despite a large variety in the position and number of mutations and types of ligands bound. Since subsequent comparison focused on the analysis of protein−ligand interaction energies and on local structural changes induced by the different mutations, a simulation time of 1 ns was considered sufficient. As shown in previous simulations of HIV-1 protease, the respective data can even be obtained from simulations on a sub-ns time scale.[50,51]

Protease-Ligand Interaction Energies. The van der Waals interaction energy between protease and ligand provides a suitable parameter to obtain first information about the role of particular sequence positions for the emergence of drug resistance.[51] A decrease of the van der Waals

Table 1: Protein-Ligand van der Waals Interaction Energies and Corresponding Standard Deviations[a]

ligand	protease	energy [kcal mol^{-1}]
SUB	WT	-83.5 ± 3.9
SUB	D30N	-79.3 ± 5.0
SUB	N88S	-78.4 ± 4.0
APV	WT	-60.7 ± 3.7
APV	D30N	-61.0 ± 3.8
APV	N88S	-61.4 ± 4.0
NLF	WT	-68.2 ± 3.2
NLF	D30N	-58.9 ± 3.5
NLF	N88S	-66.9 ± 3.7

[a] The energy was calculated using the AMBER parm99 force field and a 99 Å cutoff for all pairwise interactions. Water molecules and ions were not included. Mean energy values and standard deviations were based on a set of 1000 structures collected every ps over the entire simulation.

interaction energy in mutant proteases is indicative for a loss of the tight packing of the inhibitor in the active site resulting either from steric clashes or from the loss of favorable attractive interactions (e.g. hydrogen bonds, salt bridges). The overall values of these interaction energies were first confirmed to be not critically affected by the protonation state of the active site as shown by a control simulation for the Nelfinavir-bound wild-type protease, which yielded an interaction energy of -66.4 ± 3.6 kcal mol^{-1} compared to -68.2 ± 3.2 kcal mol^{-1} for the simulation using a fully deprotonated active site.

Assuming that a phenotypically observed decreased susceptibility is correlated with a decreased interaction energy, one would expect that the D30N and N88S mutations do not affect the interaction energies for the substrate- and Amprenavir-liganded proteases. Indeed, no significant decrease of the van der Waals interaction energy upon both mutations was observed for the substrate and Amprenavir (Table 1). For Nelfinavir, a significant decrease in binding-energy from -68.2 ± 3.2 kcal mol^{-1} to -58.9 ± 3.5 kcal mol^{-1} was observed for the D30N mutation, while the N88S mutation did not result in significant changes (Table 1).

The effect of the D30N mutation can be rationalized by inspection of the crystal structure[23] in which the carboxyl group of the D30 side chain of one subunit is critically involved in a hydrogen bond with the hydroxyl group of the aromatic ring of NLF (Figure 1; red arrow). This mechanism for resistance is supported by previous data of Wang and Kollman,[51] who also reported a decreased interaction energy for other primary, active-site mutations.

In contrast, the nonactive-site mutation N88S investigated here did not lead to a significant decrease of van der Waals interaction energy for all ligands studied (Table 1) showing that the NLF resistance caused by this mutation cannot easily be explained by simple energetic considerations of the ligand-bound proteases. Similar observations have been made in a very recent study by Chen et al.[16] in which 14 HIV-1 protease mutants complexes with the inhibitor Indinavir were characterized by MD simulations and subsequent energetic analysis. In particular for the nonactive site mutants L24I, G73S, N88D, and L90M a prediction of resistance on the basis of the dynamic properties and interaction energies proved to be difficult.[16]

Table 2: Hydrogen Bonds Observed at the Site of the Mutation[a]

protease	N/S88 − T74 (%)	N/S88 − D30 (%)
WT-NLF	94.3	0.1
WT-free	66.1	19.0
N88S-free	25.7	28.7

[a] Hydrogen bond donors are the side chain amide group of Asn88 and the side chain hydroxyl group of Ser88. Acceptor atoms are the backbone O of Thr74 and the side chain OD1 of Asp30 (Figure 4E, F). The presence of a hydrogen bond was inferred from a proton-acceptor distance of < 2.6 Å and a donor-proton-acceptor angle of $> 120°$. Values are given in percent and represent averages over both subunits and the 1 ns simulation time.

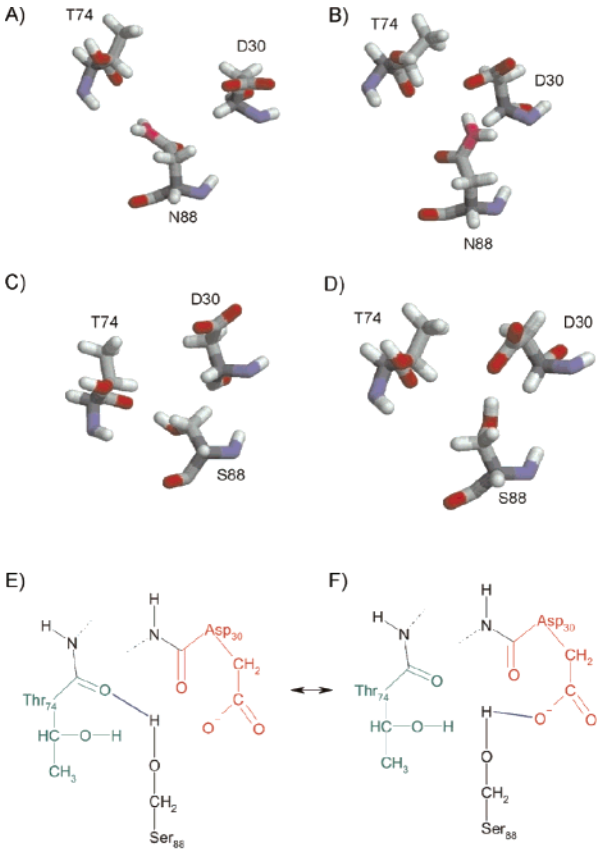

Figure 4. Alternative hydrogen bond pairs 88−30 and 88−74 in the unliganded WT and N88S mutant structures. Only the three amino acids involved are depicted in stick representation. A+B) unliganded wild-type protease, C+D) unliganded N88S mutant. The snapshots of the WT were taken at 700 and 150 ps, and for the N88S protease at $t = 250$ and 500 ps representing situations in which either the 88−74 (A+C) or the 88−30 (B+D) hydrogen bond is present. E+F) Schematic representation of the hydrogen bonds observed during MD simulation in the unliganded N88S protease. Hydrogen bonds are drawn in blue.

Comparison of Free and Ligand-Bound Structures of HIV Protease. To find an explanation for the NLF resistance of the N88S mutant, structural analysis was extended to the unbound forms of HIV-1 protease. The rationale behind this strategy is the observation that conformational sampling of

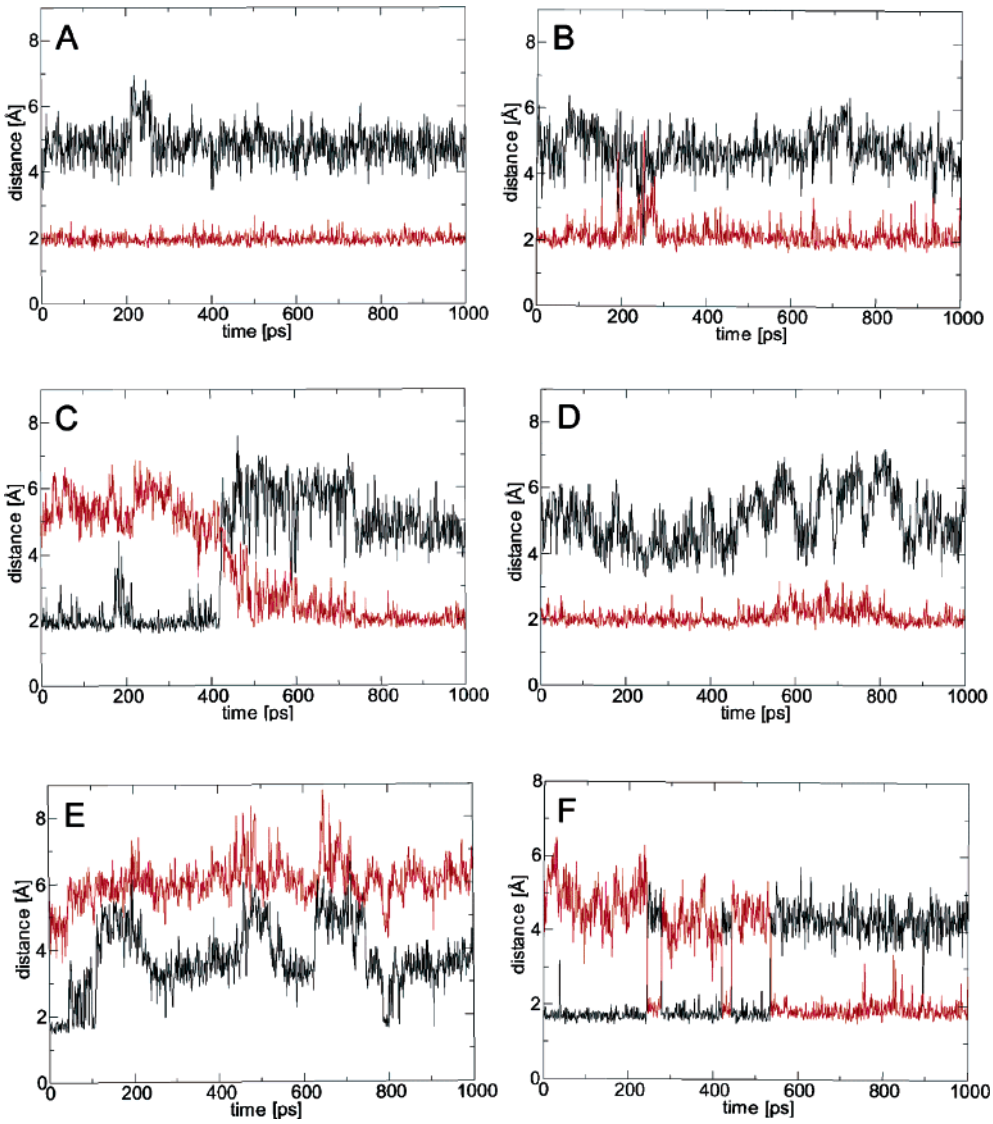

Figure 5. Distances between hydrogen bond donor and acceptor atoms of Asp30, Thr74 and Asn/Ser88 as a function of simulation time. Hydrogen bond donor atoms are side chain amide proton of Asn88 and side chain hydroxyl proton of Ser88. Acceptor atoms are backbone O of Thr 74 (red line) and side chain OD1 of Asp30 (black line). Subunit 1 (left panel), subunit 2 (right panel). A+B) WT protease liganded with NLF, C+D) unliganded WT protease, E+F) unliganded N88S protease. Analysis of the hydrogen bonding pattern was performed separately for both subunits in order to take into account the asymmetric structure of NLF. Distances of ~2 Å indicate that the groups are sufficiently close for the formation of a hydrogen bond.

proteins is frequently critically affected by mutations[52−54] and thus may also influence ligand binding affinity due to the presence of different amounts of "binding-competent" conformations.[55,56] The present analysis therefore focused on the Nelfinavir-bound wild-type protease as well as the free wild-type and free N88S mutant. Based on the considerations outlined above, one would expect that binding of the ligand is facilitated if the "binding-competent" conformation is already predefined in the unbound form of the protease.

Analysis of the structure in the region of the mutation revealed that a N88-T74 hydrogen bond exists over 94.3% of the simulation time for the Nelfinavir-bound wild-type and may thus be considered as feature of a "binding-competent" conformation. In the free wild-type and N88S protease the portion of structures exhibiting this hydrogen bond is generally lower than in the Nelfinavir-bound form but differs considerably between both free proteases (66.1% in the WT vs 25.7% in the mutant; Table 2). This difference in the population of this hydrogen bond by a factor of ~2.5 between the free wild-type and free N88S protease indicates that this mutation can actually shift the conformational equilibrium of the free protease.

Analysis of those conformations that lack the 88−74 hydrogen bond revealed that the predominant alternative hydrogen bond of residue 88 is formed to the Asp30 side chain which plays an important role for NLF binding. This role is evidenced by the fact that a replacement of Asp by Asn in the active-site D30N mutant leads to NLF resistance.[6] Analysis of the geometry of the corresponding region in the wild-type and N88S mutant (Figure 4) suggests that the 88−74 and 88−30 hydrogen bonds should be mutually exclusive. This is confirmed by monitoring the donor−acceptor distance over the simulation time (Figure 5) showing that both

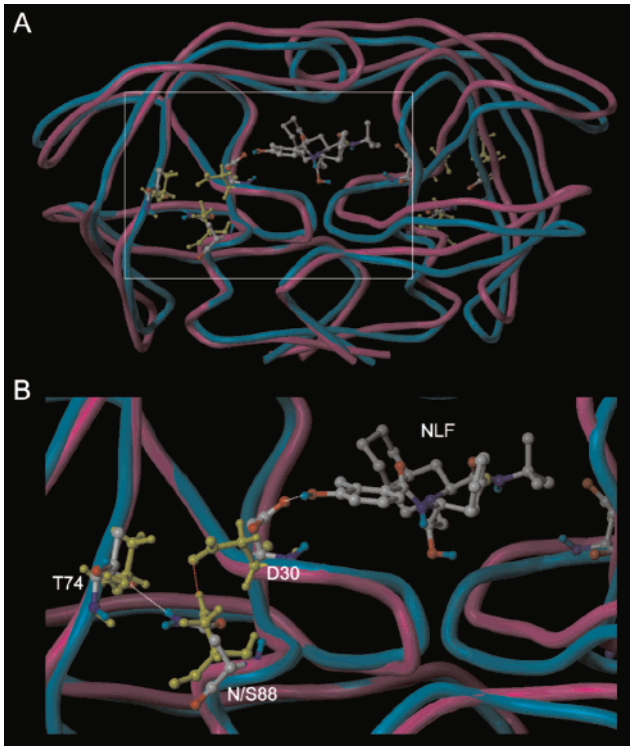

Figure 6. A) Overlay of the crystal structure of NLF-bound protease (cyan) with the structure of the free N88S mutation obtained after 300 ps in the MD simulation (magenta). Residues D30, N/S88, and T74, that are part of the hydrogen bonding network, and the inhibitor are shown in ball-and-sick representation. Residues of the NLF-bound protease are colored in cpk and those of the free N88S mutant in yellow. The part of the structure marked by the white square is shown as enlargement in B) and the alternative hydrogen bonds are indicated. White dotted lines indicate the N88-T74 and D30-NLF hydrogen bonds present in the NLF-bound wild-type, whereas a red dotted line indicates the alternative S88-D30 hydrogen bond present in the free mutant. For the latter interaction a significant rotation of the D30 side chain is observed, hampering an interaction with the inhibitor.

hydrogen bonds never exist at the same time, and a switching between both conformations is observed instead (Figure 5C, F).

Interestingly, the alternative 88−30 hydrogen bond is observed more frequently in the free N88S mutant (28.7%; Table 2) compared to the free wild-type (19.0%) offering an explanation for the resistance caused by the N88S mutation. In addition to this increase of ∼50% in the occurrence of this hydrogen bond, the N88S mutation also affects the $\chi 1$ side chain rotamer distribution of Asp30. While in the simulation of the free wild-type only the $-60°$ rotamer is observed, an alterative rotamer ($\chi 1 = \sim -150°$) is detected in the simulation of the N88S mutant when the 88−30 hydrogen bond is formed. This deviation from this $\chi 1 = -60°$ rotamer, that is also present in the Nelfinavir-bound state, has the consequence that the D30 side chain is rotated away from the ligand binding pocket in the N88S mutant (Figure 6) thus no longer providing a suitable interaction partner for NLF. The fact that such alternative rotamers are not observed in the free wild-type even when a N88-D30 hydrogen bond is formed can most likely be attributed to differences in the length and geometry of the Asp88 and Ser88 side chain. Taken together, there are three structural properties of the free N88S mutant that clearly differ from the free wild-type protease thus offering an explanation for resistance: A decrease in the frequency of the 88−74 hydrogen bond characteristic for the Nelfinavir-bound form by more than 60%, an increase of the alternative 88−30 hydrogen bond by ∼ 50%, and the observation of an alternative rotamer for D30 which is critically involved in NLF binding.

For the following reasons it can be excluded that these structural differences are an artifact resulting from the simulation or the choice of the starting structures: First, both simulations of wild-type and mutant unbound protease started from the same crystal structure and thus differ only by the presence of the N88S mutation. Second, all starting structures of the unliganded proteases were generated by removal of APV and not of NLF from a ligand-bound protease. Therefore, no information about particular structural properties of the Nelfinavir-bound form, which could result in a bias of the corresponding simulations, was "transferred" to the unbound starting structures. Third, the switching between different hydrogen bonds shows that the simulation time was sufficiently long to allow a sampling of these different conformations rendering an analysis of their relative population valid.

Thus, a conformational equilibrium exists for the HIV-1 protease, prior to binding of drug or substrate, between two populations that differ in their hydrogen bond pattern and side chain rotamers of Asp30. Due to the N88S mutation, the equilibrium is shifted toward a conformation that hampers NLF binding. This interpretation also offers an explanation for the fact that the effects of the N88S mutation could not be detected by an energetic analysis of the ligand bound form and shows that the approach of predicting resistance from analysis of ligand-bound structures alone cannot generally be applied.

The influence of a conformational-equilibrium on binding kinetics has already been described in the literature for several systems such as thrombin,[57] cAMP-dependent protein kinase,[58] and the oestrogen receptor[59] as well as aldose reductase.[55,60] Another well-studied example is the binding of SH3 domains to putative peptide ligands.[61] For this system, manifold conformations exist prior to binding, which are significantly reduced upon binding and are thus coupled to a cooperative conformational change. Recently, Perryman et al.[15] also observed a conformational equilibrium in the unliganded HIV-1 protease that is affected by mutation. In the V82F/I84V mutant differences in the curling of the protease's flap region compared to the wild-type were detected that resulted in a shift of the equilibrium between closed and semiopen conformation, thus offering a plausible explanation for the drug resistance mechanism of this mutant. Hence, this study is in accordance with the present findings suggesting that conformational equilibria might generally play a role for ligand binding and emergence of resistance for HIV-1 protease.

The mechanism suggested by the present study in which alternative hydrogen bonding patterns play an important role may also apply to other nonactive site mutations, for example for L90M which also directly confers resistance although it does not directly contact the ligand. Analysis of protease crystal structures containing the L90M mutation[62,63] reveals that the sulfur atom of the methionine is in close spatial proximity to the active-site residue D25 which is critically involved in ligand binding. Therefore, one could envisage a mode of action similar to the N88S mutant in which the sulfur of M90, that has no equivalent in the wild-type L90, could function as a novel hydrogen bond acceptor and thus interfere with the hydrogen bonding network present in wild-type protease.

More, and possibly also longer MD simulations, will be necessary for a comprehensive investigation of the role of unbound conformations in the emergence of resistance caused by nonactive-site mutations and thus will help to design novel and more effective drugs, e.g. by targeting different residues or by developing allosteric inhibitors that are capable of regulating protease dynamics.

Acknowledgment. We thank the Computer-Chemie-Centrum Erlangen for support with the Gaussian calculations.

References

(1) UNAIDS/WHO *2004 Report on the global AIDS epidemic*; **2004**.

(2) Kohl, N. E.; Emmi, E. A.; Schleif, W. A.; Davies, L. J.; Heimbach, J. C.; Dixon, R. A. F. Active human immunodeciency virus protease is required for viral infectivity. *Proc. Natl. Acad. Sci.* **1988**, *85*, 686−690.

(3) Katoh, I.; Yasunaga, T.; Ikawa, Y.; Yoshinaka, Y. Inhibition of retroviral protease activity by an aspartyl proteinase inhibitor. *Nature* **1987**, *329*, (6140), 654−6.

(4) Stephenson, J. The art of 'HAART': researchers probe the potential and limits of aggressive HIV treatments. *Jama* **1997**, *277*, (8), 614−6.

(5) Voelker, R. The world in medicine: HIV drug resistance. *Jama* **2000**, *284*, (2), 169.

(6) Shafer, R. W. Genotypic testing for human immunodeficiency virus type 1 drug resistance. *Clin. Microbiol. Rev.* **2002**, *15*, (2), 247−77.

(7) Draghici, S.; Potter, R. B. Predicting HIV drug resistance with neural networks. *Bioinformatics* **2003**, *19*, (1), 98−107.

(8) Piana, S.; Carloni, P.; Röthlisberger, U. Drug resistance in HIV-1 protease: Flexibility-assisted mechanism of compensatory mutations. *Protein Sci.* **2002**, *11*, (10), 2393−402.

(9) Muzammil, S.; Ross, P.; Freire, E. A major role for a set of nonactive site mutations in the development of HIV-1 protease drug resistance. *Biochemistry* **2003**, *42*, (3), 631−8.

(10) Walter, H.; Schmidt, B.; Korn, K.; Vandamme, A. M.; Harrer, T.; Uberla, K. Rapid, phenotypic HIV-1 drug sensitivity assay for protease and reverse transcriptase inhibitors. *J. Clin. Virol.* **1999**, *13*, (1−2), 71−80.

(11) Martinez-Picado, J.; Savara, A. V.; Shi, L.; Sutton, L.; D'Aquila, R. T. Fitness of human immunodeficiency virus type 1 protease inhibitor-selected single mutants. *Virology* **2000**, *275*, (2), 318−22.

(12) Schmidt, B.; Walter, H.; Moschik, B.; Paatz, C.; van Vaerenbergh, K.; Vandamme, A. M.; Schmitt, M.; Harrer, T.; Uberla, K.; Korn, K. Simple algorithm derived from a geno-/phenotypic database to predict HIV-1 protease inhibitor resistance. *Aids* **2000**, *14*, (12), 1731−8.

(13) Schinazi, R. F.; Larder, B.; Mellors, J. W. Mutations in retroviral genes associated with drug resistance: 2000−2001 update. *Int. Antivir. News* **2000**, *8*, 65−92.

(14) Blaise, P.; Clevenbergh, P.; Vaira, D.; Moutschen, M.; Dellamonica, P. HIV resistance to antiretroviral drugs: mechanisms, genotypic and phenotypic resistance testing in clinical practice. *Acta Clin. Belg.* **2002**, *57*, (4), 191−201.

(15) Perryman, A. L.; Lin, J. H.; McCammon, J. A. HIV-1 protease molecular dynamics of a wild-type and of the V82F/I84V mutant: possible contributions to drug resistance and a potential new target site for drugs. *Protein Sci.* **2004**, *13*, (4), 1108−23.

(16) Chen, X.; Weber, I. T.; Harrison, R. W. Molecular dynamics simulations of 14 HIV protease mutants in complexes with indinavir. *J. Mol. Model. (Online)* **2004**, *10*, (5−6), 373−81.

(17) Markowitz, M.; Conant, M.; Hurley, A.; Schluger, R.; Duran, M.; Peterkin, J.; Chapman, S.; Patick, A.; Hendricks, A.; Yuen, G. J.; Hoskins, W.; Clendeninn, N.; Ho, D. D. A preliminary evaluation of nelfinavir mesylate, an inhibitor of human immunodeficiency virus (HIV)-1 protease, to treat HIV infection. *J. Infect. Dis.* **1998**, *177*, (6), 1533−40.

(18) Petropoulos, C. J.; Parkin, N. T.; Limoli, K. L.; Lie, Y. S.; Wrin, T.; Huang, W.; Tian, H.; Smith, D.; Winslow, G. A.; Capon, D. J.; Whitcomb, J. M. A novel phenotypic drug susceptibility assay for human immunodeficiency virus type 1. *Antimicrob. Agents Chemother.* **2000**, *44*, (4), 920−8.

(19) Ziermann, R.; Limoli, K.; Das, K.; Arnold, E.; Petropoulos, C. J.; Parkin, N. T. A mutation in human immunodeficiency virus type 1 protease, N88S, that causes in vitro hypersensitivity to amprenavir. *J. Virol.* **2000**, *74*, (9), 4414−9.

(20) Patick, A. K.; Duran, M.; Cao, Y.; Shugarts, D.; Keller, M. R.; Mazabel, E.; Knowles, M.; Chapman, S.; Kuritzkes, D. R.; Markowitz, M. Genotypic and phenotypic characterization of human immunodeficiency virus type 1 variants isolated from patients treated with the protease inhibitor nelfinavir. *Antimicrob. Agents Chemother.* **1998**, *42*, (10), 2637−44.

(21) Berman, H. M.; Westbrook, J.; Feng, Z.; Gilliland, G.; Bhat, T. N.; Weissig, H.; Shindyalov, I. N.; Bourne, P. E. The Protein Data Bank. *Nucleic Acids Res.* **2000**, *28*, (1), 235−42.

(22) Kim, E. E.; Baker, C. T.; Dwyer, M. D.; Murcko, M. A.; Rao, B. G.; Tung, R. D.; Navia, M. A. Crystal Structure of HIV-1 Protease in Complex with VX-478, a potent and orally bioavailable Inhibitor of the Enzyme. *J. Am. Chem. Soc.* **1995**, *117*, 1181−1182.

(23) Kaldor, S. W.; Kalish, V. J.; Davies, J. F., II; Shetty, B. V.; Fritz, J. E.; Appelt, K.; Burgess, J. A.; Campanale, K. M.; Chirgadze, N. Y.; Clawson, D. K.; Dressman, B. A.; Hatch, S. D.; Khalil, D. A.; Kosa, M. B.; Lubbehusen, P. P.; Muesing, M. A.; Patick, A. K.; Reich, S. H.; Su, K. S.; Tatlock, J. H. Viracept (nelfinavir mesylate, AG1343): a potent, orally bioavailable inhibitor of HIV-1 protease. *J. Med. Chem.* **1997**, *40*, (24), 3979−85.

(24) Miller, M.; Schneider, J.; Sathyanarayana, B. K.; Toth, M. V.; Marshall, G. R.; Clawson, L.; Selk, L.; Kent, S. B.; Wlodawer, A. Structure of complex of synthetic HIV-1 protease with a substrate-based inhibitor at 2.3 A resolution. *Science* **1989**, *246*, (4934), 1149−52.

(25) Kurt, N.; Scott, W. R.; Schiffer, C. A.; Haliloglu, T. Cooperative fluctuations of unliganded and substrate-bound HIV-1 protease: a structure-based analysis on a variety of conformations from crystallography and molecular dynamics simulations. *Proteins* **2003**, *51*, (3), 409−22.

(26) Dolezal, O.; De Gori, R.; Walter, M.; Doughty, L.; Hattarki, M.; Hudson, P. J.; Kortt, A. A. Single-chain Fv multimers of the anti-neuraminidase antibody NC10: the residue at position 15 in the V(L) domain of the scFv-0 (V(L)-V(H)) molecule is primarily responsible for formation of a tetramer-trimer equilibrium. *Protein Eng.* **2003**, *16*, (1), 47−56.

(27) Chen, Y. Z.; Gu, X. L.; Cao, Z. W. Can an optimization/scoring procedure in ligand-protein docking be employed to probe drug-resistant mutations in proteins? *J. Mol. Graph. Model.* **2001**, *19*, 450−570.

(28) Tripos *Sybyl 6.9, Release 7.0A.*, St. Louis, Missouri, USA, 1991−2002.

(29) Ratner, L.; Haseltine, W.; Patarca, R.; Livak, K. J.; Starcich, B.; Josephs, S. F.; Doran, E. R.; Rafalski, J. A.; Whitehorn, E. A.; Baumeister, K.; et al. Complete nucleotide sequence of the AIDS virus, HTLV−III. *Nature* **1985**, *313*, (6000), 277−84.

(30) Tie, Y.; Boross, P. I.; Wang, Y. F.; Gaddis, L.; Hussain, A. K.; Leshchenko, S.; Ghosh, A. K.; Louis, J. M.; Harrison, R. W.; Weber, I. T. High-resolution crystal structures of HIV-1 protease with a potent non-peptide inhibitor (UIC-94017) active against multi-drug-resistant clinical strains. *J. Mol. Biol.* **2004**, *338*, (2), 341−52.

(31) Smith, R.; Brereton, I. M.; Chai, R. Y.; Kent, S. B. Ionization states of the catalytic residues in HIV-1 protease. *Nat. Struct. Biol.* **1996**, *3*, (11), 946−50.

(32) Thomson, M. A. *Arguslab 3.1*, Planaria Software LLC: Seattle, WA, 2004.

(33) Rappé, A. K.; Casewit, C. J.; Colwell, K. S.; Goddard, W. A. I.; Skiff, W. M. UFF, a Rule-Based Full Periodic Table Force Field for Molecular Mechanics and Molecular Dynamics Simulations. *J. Am. Chem. Soc.* **1992**, *114*, 10024−10035.

(34) Dewar, M. J. S.; Zoebisch, E. G.; Healy, E. F.; Stewart, J. J. P. AM1: A New General Purpose Quantum Mechanical Molecular Model. *J. Am. Chem. Soc.* **1985**, *107*, 3902−3909.

(35) Clark, T.; Alex, A.; Beck, B.; Burkhardt, F.; Chandrasekhar, J.; Gedeck, P.; Horn, A. H. C.; Hutter, M.; Martin, B.; Rauhut, G.; Sauer, W.; Schindler, T.; Steinke, T. *Vamp8.1 B33*, Erlangen, 2000−2004.

(36) Frisch, M. J.; Trucks, G. W.; Schlegel, H. B.; Scuseria, G. E.; Robb, M. A.; Cheeseman, J. R.; Zakrzewski, V. G.; Montgomery, J. A., Jr.; Stratmann, R. E.; Burant, J. C.; Dapprich, S.; Millam, J. M.; Daniels, A. D.; Kudin, K. N.; Strain, M. C.; Farkas, O.; Tomasi, J.; Barone, V.; Cossi, M.; Cammi, R.; Mennucci, B.; Pomelli, C.; Adamo, C.; Clifford, S.; Ochterski, J.; Petersson, G. A.; Ayala, P. Y.; Cui, Q.; Morokuma, K.; Malick, D. K.; Rabuck, A. D.; Raghavachari, K.; Foresman, J. B.; Cioslowski, J.; Ortiz, J. V.; Baboul, A. G.; Stefanov, B. B.; Liu, G.; Liashenko, A.; Piskorz, P.; Komaromi, I.; Gomperts, R.; Martin, R. L.; Fox, D. J.; Keith, T.; Al-Laham, M. A.; Peng, C. Y.; Nanayakkara, A.; Gonzalez, C.; Challacombe, M.; Gill, P. M. W.; Johnson, B.; Chen, W.; Wong, M. W.; Andres, J. L.; Gonzalez, C.; Head-Gordon, M.; Replogle, E. S.; Pople, J. A. *Gaussian 98, Revision A.11.3*, Gaussian Inc.: Pittsburgh, PA, 1998.

(37) Bayly, C. I.; Cieplak, P.; Cornell, W. D.; Kollman, P. A. A well-behaved electrostatic potential based method using charge restraints for deriving atomic charges: the RESP model. *J. Phys. Chem.* **1993**, *97*, 10269−10280.

(38) Cornell, W. D.; Cieplak, P.; Bayly, C. I.; Kollman, P. A. Application of RESP charges to calculate conformational energies, hydrogen bond energies and free energies of solvation. *J. Am. Chem. Soc.* **1993**, *115*, 9620−9631.

(39) Pearlman, D. A.; Case, D. A.; Caldwell, J. W.; Ross, W. S.; Cheatham, T. E., III; DeBolt, S.; Ferguson, D.; Seibel, G.; Kollman, P. AMBER, a package of computer programs for applying molecular mechanics, normal-mode analysis, molecular dynamics and free energy calculations to simulate the structural and energetic properties of molecules. *Comput. Phys. Commun.* **1995**, *91*, 1−41.

(40) Cornell, W. D.; Cieplak, P.; Bayly, C. I.; Gould, I. R.; Merz, K. M. J.; Ferguson, D. M.; Spellmeyer, D. C.; Fox, T.; Caldwell, J. W.; Kollman, P. A. A Second Generation Force Fiel for the Simulaton of Proteins, Nucleic Acids and Organic Molecules. *J. Am. Chem. Soc.* **1995**, *117*, 5179−5197.

(41) Cheatham, T. E., III; Cieplak, P.; Kollman, P. A. A modified version of the Cornell et al. force field with improved sugar pucker phases and helical repeat. *J. Biomol. Struct. Dyn.* **1999**, *16*, (4), 845−62.

(42) Wang, J.; Wolf, R. M.; Caldwell, J. W.; Kollman, P. A.; Case, D. A. Development and testing of a general amber force field. *J. Comput. Chem.* **2004**, *25*, (9), 1157−74.

(43) Jorgensen, W. L.; Chandrasekhar, J.; Madura, J. D.; Impey, R. W.; Klein, M. L. Comparison of simple potential functions for simulating liquid water. *J. Chem. Phys.* **1983**, *79*, 926−935.

(44) Darden, T. A.; York, D. M.; Pedersen, L. G. Particle mesh Ewald. An N.log(N) method for Ewald sums in large systems. *J. Chem. Phys.* **1993**, *98*, 10089−10092.

(45) Ryckaert, J. P.; Ciccotti, G.; Berendsen, H. J. C. Numerical integration of the Cartesian equations of motion of a system with constraints: molecular dynamics of *n*-alkanes. *J. Comput. Phys.* **1977**, *23*, 327−341.

(46) Sayle, R. A.; Milner-White, E. J. RASMOL: biomolecular graphics for all. *Trends Biochem. Sci.* **1995**, *20*, (9), 374.

(47) MDL *ISIS/Draw 2.3.*, San Leandro, CA, 1990−2000.

(48) Brünger, A. T. XPLOR, version 3.1. A system for X-ray crystallography and NMR. *Yale University Press: New Haven, CT* **1992**.

(49) Lepsik, M.; Kriz, Z.; Havlas, Z. Efficiency of a second-generation HIV-1 protease inhibitor studied by molecular dynamics and absolute binding free energy calculations. *Proteins* **2004**, *57*, (2), 279−93.

(50) Zoete, V.; Michielin, O.; Karplus, M. Relation between sequence and structure of HIV-1 protease inhibitor complexes: a model system for the analysis of protein flexibility. *J. Mol. Biol.* **2002**, *315*, (1), 21−52.

(51) Wang, W.; Kollman, P. A. Computational study of protein specificity: the molecular basis of HIV-1 protease drug resistance. *Proc. Natl. Acad. Sci. U.S.A.* **2001**, *98*, (26), 14937−42.

(52) Tsai, C. J.; Ma, B.; Nussinov, R. Folding and binding cascades: shifts in energy landscapes. *Proc. Natl. Acad. Sci. U.S.A.* **1999**, *96*, (18), 9970−2.

(53) Luque, I.; Freire, E. Structural stability of binding sites: consequences for binding affinity and allosteric effects. *Proteins* **2000**, *Suppl 4*, 63−71.

(54) Sinha, N.; Nussinov, R. Point mutations and sequence variability in proteins: redistributions of preexisting populations. *Proc. Natl. Acad. Sci. U.S.A.* **2001**, *98*, (6), 3139−44.

(55) Davis, A.; Teague, S. Hydrogen bonding, hydrophobic interactions, and failure of the rigid receptor hypothesis. *Angew. Chem., Int. Ed. Engl.* **1999**, *38*, 736−749.

(56) Rauh, D.; Klebe, G.; Stubbs, M. T. Understanding protein−ligand interactions: the price of protein flexibility. *J. Mol. Biol.* **2004**, *335*, (5), 1325−41.

(57) Engh, R. A.; Brandstetter, H.; Sucher, G.; Eichinger, A.; Baumann, U.; Bode, W.; Huber, R.; Poll, T.; Rudolph, R.; von der Saal, W. Enzyme flexibility, solvent and 'weak' interactions characterize thrombin-ligand interactions: implications for drug design. *Structure* **1996**, *4*, (11), 1353−62.

(58) Prade, L.; Engh, R. A.; Girod, A.; Kinzel, V.; Huber, R.; Bossemeyer, D. Staurosporine-induced conformational changes of cAMP-dependent protein kinase catalytic subunit explain inhibitory potential. *Structure* **1997**, *5*, (12), 1627−37.

(59) Brzozowski, A. M.; Pike, A. C.; Dauter, Z.; Hubbard, R. E.; Bonn, T.; Engstrom, O.; Ohman, L.; Greene, G. L.; Gustafsson, J. A.; Carlquist, M., Molecular basis of agonism and antagonism in the oestrogen receptor. *Nature* **1997**, *389*, (6652), 753−8.

(60) Urzhumtsev, A.; Tete-Favier, F.; Mitschler, A.; Barbanton, J.; Barth, P.; Urzhumtseva, L.; Biellmann, J. F.; Podjarny, A.; Moras, D. A 'specificity' pocket inferred from the crystal structures of the complexes of aldose reductase with the pharmaceutically important inhibitors tolrestat and sorbinil. *Structure* **1997**, *5*, (5), 601−12.

(61) Ferreon, J. C.; Hilser, V. J. Ligand-induced changes in dynamics in the RT loop of the C-terminal SH3 domain of Sem-5 indicate cooperative conformational coupling. *Protein Sci.* **2003**, *12*, (5), 982−96.

(62) Clemente, J. C.; Moose, R. E.; Hemrajani, R.; Whitford, L. R.; Govindasamy, L.; Reutzel, R.; McKenna, R.; Agbandje-McKenna, M.; Goodenow, M. M.; Dunn, B. M. Comparing the accumulation of active- and nonactive-site mutations in the HIV-1 protease. *Biochemistry* **2004**, *43*, (38), 12141−51.

(63) Mahalingam, B.; Wang, Y. F.; Boross, P. I.; Tozser, J.; Louis, J. M.; Harrison, R. W.; Weber, I. T. Crystal structures of HIV protease V82A and L90M mutants reveal changes in the indinavir-binding site. *Eur. J. Biochem.* **2004**, *271*, (8), 1516−24.

CT049869O